

New Measurement of the  $\pi^+ \rightarrow e\nu$  Branching Ratio

D.A. Bryman, R. Dubois,<sup>(a)</sup> T. Numa, B. Olaniyi,<sup>(b)</sup> and A. Giin  
TRIUMF and University of Victoria, Vancouver, B.C., Canada V6T 2A3

and

M.S. Dixit

National Research Council of Canada, Ottawa, Canada K1A 0R6

and

D. Berghofer and J-M. Poutissou  
TRIUMF and University of British Columbia  
Vancouver, B.C., Canada V6T 2A3

and

J.A. Macdonald  
TRIUMF, Vancouver, B.C., Canada V6T 2A3

and

B.C. Robertson  
Queen's University, Kingston, Ontario, Canada K7L 3N6

## Abstract

A new measurement of the  $\pi^+ \rightarrow e\nu$  branching ratio yields

$$\frac{\Gamma(\pi^+ \rightarrow e\nu + \pi^+ e\nu\gamma)}{\Gamma(\pi^+ \rightarrow \mu\nu + \pi^+ \mu\nu\gamma)} = (1.218 \pm 0.014) \times 10^{-4}.$$

The measured value is in good agreement with the standard model prediction incorporating electron-muon universality.

(submitted to Physical Review Letters)

A major puzzle in particle physics involves the existence of multiple seemingly redundant generations of fundamental particles. The lepton generations apparently have identical electromagnetic interactions as evidenced by the agreement of experiments and theory on the values of electron and muon anomalous magnetic moments. The hypothesis of universality of the weak interaction is tested most stringently using the branching ratio for the electronic and muonic decay modes of the pion. The theoretical value of the branching ratio including radiative corrections

$$R \equiv \frac{\Gamma(\pi \rightarrow e\nu + \pi \rightarrow e\nu\gamma)}{\Gamma(\pi \rightarrow \mu\nu + \pi \rightarrow \mu\nu\gamma)}$$
$$= 1.233 \left( \frac{f_{\pi}^e}{f_{\pi}^{\mu}} \right)^2 \times 10^{-4} \quad (1)$$

was determined by Kinoshita<sup>1</sup> in an early (V,A) phenomenological calculation where  $f_{\pi}^{\ell}$  is the pion decay constant and  $f_{\pi}^e = f_{\pi}^{\mu}$  if universality holds. This result was reaffirmed to the level  $\pm 0.5\%$  in the context of the standard gauge theory of weak and electromagnetic interactions by the theorem on radiative corrections in  $\pi_{\ell 2}$  decay proved by Marciano and Sirlin<sup>2</sup> and by specific model calculations by Goldman and Wilson.<sup>3</sup> An early measurement<sup>4</sup> by Anderson et al.<sup>5</sup> found  $R = (1.21 \pm 0.07) \times 10^{-4}$  in agreement with Eq. (1). Subsequently, an experiment by Di Capua et al.<sup>6</sup> obtained<sup>7</sup>  $R = (1.274 \pm 0.024) \times 10^{-4}$  which differs from the theoretical prediction by  $(3.3 \pm 1.9)\%$ . In this letter, a new measurement of the branching ratio is reported.

The experiment was performed in a pion beam at the Tri-University Meson Facility (TRIUMF) in Vancouver, Canada. The set-up is shown in Fig. 1. Positive pions with initial momentum  $p_{\pi} = 77 \pm 1$  MeV/c were degraded and stopped at a rate of  $2 \times 10^5$  s<sup>-1</sup> in the inner three layers of

a five-layer scintillation counter target designed to absorb all muons from  $\pi^+ \rightarrow \mu^+ \nu_\mu$  decay. 70 MeV positrons from  $\pi^+ \rightarrow e^+ \nu_e$  decay and 0-53 MeV positrons from the  $\pi-\mu-e$  decay chain ( $\pi^+ \rightarrow \mu^+ \nu_\mu$  followed by  $\mu^+ \rightarrow e^+ \nu_e \bar{\nu}_\mu$ ) were detected by a three-element scintillation counter telescope (T1, T2, T3) which preceded the 46 cm  $\phi \times 51$  cm NaI(Tl) crystal TINA. T3 limited the positron solid angle acceptance to  $\Delta\omega/4\pi = 0.7\%$  so that the measurements were confined to the central portion of the crystal for best energy resolution and to avoid edge effects. Three multi-wire proportional chambers (MWPC 1-3) were used to test for position-dependent systematic effects.

Since NaI detectors are sensitive to both charged particles and gamma rays, the energy measurement included internal bremsstrahlung photons which are emitted generally in the direction of the positrons in  $\pi_{e2}$  and  $\mu$  decays. The response function of the NaI crystal with its characteristic low-energy tail was measured using the positron beam component of the pion channel in the momentum range 20-90 MeV/c. At 70 MeV/c the observed resolution was  $\Delta E/E = 3.5\%$  (FWHM).

In addition to the energy measurement, the time of decay into T3 within  $\pm 200$  ns of the pion stop was recorded for each event along with energy losses ( $dE/dx$ ) in T1-T3 and several pulse pile-up times. Pile-up of additional beam particles within  $\pm 5$   $\mu$ s of the pion stop and charged particle pile-up in the counter T2 within  $\pm 5$   $\mu$ s of the decay event were recorded. These measurements facilitated study of backgrounds and time-dependent systematic effects.

The branching ratio was determined using two procedures chosen to minimize systematic uncertainties. In the method of Di Capua et al. (Ref. 6), positrons were detected during two identical 25 ns long time intervals, Bin 1 starting at  $t_0 = 3$  ns after the arrival of the pion

and Bin 2 beginning  $t_B = 173.5$  ns, or 6.7 pion lifetimes, later. Because the pion lifetime  $\tau_\pi = 26$  ns is short compared to the muon lifetime  $\tau_\mu = 2200$  ns, Bin 2 contains essentially only positrons from the  $\pi\text{-}\mu\text{-}e$  chain ( $N(2)_{\pi\mu e}$ ) whereas Bin 1 contains events from both  $\pi\text{-}\mu\text{-}e$  ( $N(1)_{\pi\mu e}$ ) and  $\pi + e\nu$  ( $N_{\pi e}$ ) origins. The branching ratio can then be expressed as

$$R = \frac{\lambda_\mu}{\lambda_\pi - \lambda_\mu} \frac{N_{\pi e}(1 - e^{-(\lambda_\pi - \lambda_\mu)t_B})}{N(2)_{\pi\mu e} e^{\lambda_\mu t_B} - N(1)_{\pi\mu e}}, \quad (2)$$

where  $\lambda_\pi$  and  $\lambda_\mu$  are the pion and muon decay rates, respectively. This method of determining R is independent of several important sources of possible uncertainties including the displacement of the first interval from the arrival time of the pion  $t_0$ , the positron detector solid angle, the absolute width of the two time bins (as long as they are identical) and the fraction of muons in the beam or the contribution from decays of muons left in the target by previous pion stops.

Figure 2(a) shows the positron energy spectrum for Bin 1 including the  $\pi^+ + e^+ \nu_e$  peak and  $\mu^+ + e^+ \nu_e \bar{\nu}_\mu$  spectrum which extends to zero observed energy since the NaI pulse was not required in the event logic. The two low energy peaks are due to the zero energy pedestal and the 511 keV positron annihilation line. Figure 2(b) gives the pure  $\mu^+ + e^+ \nu_e \bar{\nu}_\mu$  spectrum from Bin 2. Figure 3 shows the resultant  $\pi^+ + e^+ \nu_e$  spectrum in the peak region obtained by subtracting the normalized Bin 2 muon decay distribution from Bin 1. The solid line in Fig. 3 is a fit to the data with the Monte Carlo generated  $\pi^+ + e^+ \nu_e$  lineshape (see below). The chi-squared is 1.1 per degree of freedom. The measured peak width is  $\Delta E/E \sim 5.5\%$ , in good agreement with the Monte Carlo calculation. There are  $N_{\pi e} = 3.2 \times 10^4$  counts in the peak with  $E > 51$  MeV.

The second method for calculation of the branching ratio used the two spectra in Figs. 4(a) and 4(b) which show the time distributions for events in the  $\pi$ - $\mu$ -e region and the  $\pi \rightarrow e\nu$  peak region, respectively. Events which occur prior to the arrival of the pion ( $t=0$ ) are due to decays of muons left in the target by previous pion stops. The timing spectra were fitted (solid lines) for the amplitudes of the  $\pi \rightarrow e$ ,  $\pi \rightarrow \mu \rightarrow e$  and pure  $\mu \rightarrow e$  decay contributions  $A_{\pi e}$ ,  $A_{\pi\mu e}$  and  $A_{\mu e}$ . Small additional terms were included to account for effects of pile-up and pulse-pair resolution of the scintillators. The branching ratio is given by

$$R = \frac{A_{\pi e}}{A_{\pi\mu e}} . \quad (3)$$

Chi-squared of 1.2 per degree of freedom was obtained in both fits shown as solid lines in Figs. 4(a) and 4(b). When the pion lifetime  $\tau_{\pi}$  was also a parameter in the fit, it was found that  $\tau_{\pi} = 26.10 \pm 0.13$  ns which agrees with the current value  $\tau_{\pi} = 26.030 \pm 0.023$  ns.<sup>8</sup> This method for determining R makes use of data in a wider time range than just Bins 1 and 2. However, it may be subject to additional uncertainties arising, for example, from non-linearities in the time-measuring system.

To determine the branching ratio using the two methods described, several corrections are required. Table I lists the correction factors for Eq. (2). A similar set applies to Eq. (3). The  $\pi \rightarrow e\nu$  tail correction accounts for  $\pi \rightarrow e\nu$  events lost below the 51 MeV cut-off energy. It was determined by Monte Carlo calculation of the  $\pi \rightarrow e\nu$  lineshape including the effects of the intrinsic NaI response function, radiative corrections, Bhabha scattering, Landau straggling, and the beam-target-detector geometry (see Fig. 3). Monte Carlo calculations were also done to

determine the NaI response function for  $\pi$ - $\mu$ -e chain events and to obtain other corrections including those applying to the energy dependence of processes such as multiple Coulomb scattering and positron annihilation. Small non-uniformities in the application and efficiency of pile-up cuts were determined from the data itself. The data set was tested under a series of cuts resulting in the estimated uncertainties given in Table I.

The final value of the branching ratio obtained using Eq. (2) is

$$R = (1.218 \pm 0.014) \times 10^{-4} . \quad (4)$$

A consistent result  $R = (1.219 \pm 0.014) \times 10^{-4}$  is found from the analysis method using Eq. (3).

The result Eq. (4) is in substantial agreement with the predictions of the standard model of weak and electromagnetic interactions assuming electron-muon universality. A quantitative test of universality can be obtained by comparing Eq. (4) with the theoretical prediction  $R_{th} = 1.233 \times 10^{-4}$  given in Eq. (1). It is found that

$$\frac{f_{\pi}^e}{f_{\pi}^{\mu}} = (0.9939 \pm 0.0057) . \quad (5)$$

A limit on the contribution of a pseudoscalar coupling to  $\pi_{\ell 2}$  decay can also be deduced:

$$f_p = (-0.0061 \pm 0.0057) f_{\pi} m_e . \quad (6)$$

Limits on masses of hypothetical particles contributing to pseudoscalar interactions in  $\pi_{\ell 2}$  decay have been obtained by Shanker.<sup>9</sup> For example, Eq. (6) implies a mass limit  $m_H > 350$  GeV for charged Higgs particles contributing to  $\pi_{\ell 2}$  decay in models where Higgs-fermion couplings are proportional to heavy fermion masses. Deviations from Eq. (1) may also occur in models which include massive neutrinos.<sup>10</sup> Constraints on the existence of massive neutrinos derived from the present data set will be discussed in a separate publication.<sup>11</sup>

We wish to thank G. Mason and W. Sperry for their participation in an early phase of this work and C.E. Picciotto for helpful discussions. The experiment was supported by a grant from the Natural Sciences and Engineering Research Council of Canada.

### References

(a) Present address: Stanford Linear Accelerator Center, Stanford, CA 94305

(b) Present address: University of Ife, Ile-Ife, Nigeria.

<sup>1</sup>T. Kinoshita, Phys. Rev. Lett. 2, 477 (1959).

See also S. Berman, Phys. Rev. Lett. 1, 468 (1958), R.E. Marshak, Riazuddin and C.P. Ryan, Theory of Weak Interactions in Particle Physics (Wiley-Interscience, New York, 1969), and D. Bryman, P. Depommier, and C. Leroy, Phys. Lett. C (Physics Reports), to be published.

<sup>2</sup>W. Marciano and A. Sirlin, Phys. Rev. Lett. 36, 1425 (1976).

<sup>3</sup>T. Goldman and W. Wilson, Phys. Rev. D 15, 709 (1977).

<sup>4</sup>The first observations of  $\pi^+ \rightarrow e\nu$  decay were reported by T. Fazzini, G. Fidecaro, A.W. Merrison, H. Paul, and A.U. Tollestrup, Phys. Rev. Lett. 1, 247 (1958) and G. Impeduglia, R. Plano, A. Prodell, N. Samios, M. Schwartz, and J. Steinberger, Phys. Rev. Lett. 1, 249 (1958).

<sup>5</sup>H.L. Anderson, T. Fujii, R.H. Miller, and L. Tau, Phys. Rev. 119, 2050 (1960).

<sup>6</sup>E. Di Capua, R. Garland, L. Pondrom, and A. Strelzoff, Phys. Rev. 133, B1333 (1964).

<sup>7</sup>D. Bryman and C. Picciotto, Phys. Rev. D 11, 1337 (1975).

- <sup>8</sup>Particle Data Group, Rev. Mod. Phys. 52, 568 (1980).
- <sup>9</sup>O. Shanker, Nucl. Phys. B204, 375 (1982).
- See also J.F. Donoghue and L.F. Li, Phys. Rev. D 19, 945 (1979);  
H.E. Haber, G.L. Kane, and T. Sterling, Nucl. Phys. B161, 493 (1979);  
B. McWilliams and L.F. Li, Nucl. Phys. B179, 62 (1981).
- <sup>10</sup>See R.E. Shrock, Phys. Rev. D 24, 1232 (1981).
- <sup>11</sup>D. Bryman, R. Dubois, T. Numa, B. Olaniyi, A. Olin, M.S. Dixit, J-M. Poutissou, and J.A. Macdonald, to be published.

Table I. Multiplicative corrections to  $\pi \rightarrow e\nu$  branching ratio

---

$\pi \rightarrow e\nu$ tail	$1.0147 \pm 0.0075$
Low-energy $\mu \rightarrow e\nu\nu$	$0.9982 \pm 0.0005$
Multiple Coulomb scattering	$0.9977 \pm 0.0040$
Positron annihilation	$0.9959 \pm 0.0010$
$\mu^+$ losses from target	$1.0002 \pm 0.0010$
Bin 1 and Bin 2 equality	$0.9989 \pm 0.0004$
Pulse pile-up efficiency	$0.9931 \pm 0.0029$
Bin separation $t_g$	$1.0000 \pm 0.0000$
Pion lifetime	$1.0000 \pm 0.0009$
Other	$1.0004 \pm 0.0020$

---



Figure captions

1. Set-up for the TRIUMF  $\pi^+ \rightarrow e\nu$  experiment. Scintillators B1-B8 detect pion stops, T1-T3 detect decay positrons and TINA is the large NaI(Tl) crystal described in the text.
2. (a) Observed decay positron energy spectrum for Bin 1 ( $t = 3$  to 28 ns).  
(b) Observed decay positron energy spectrum for Bin 2 ( $t = 176.5$  to 201.5 ns).
3. The  $\pi^+ \rightarrow e^+ \nu_e$  spectrum after  $\mu^+ \rightarrow e^+ \nu_e \bar{\nu}_\mu$  subtraction. The solid line is a fit of the Monte-Carlo generated lineshape to the data.
4. Timing spectra and fits (solid lines). (a)  $\pi^+ \rightarrow \mu^+ e$  events in the range 0-53 MeV, (b)  $\pi^+ \rightarrow e \nu_e$  events in the range  $>53$  MeV. A pile-up background due to  $\pi^+ \rightarrow \mu^+ e$  events was also present.

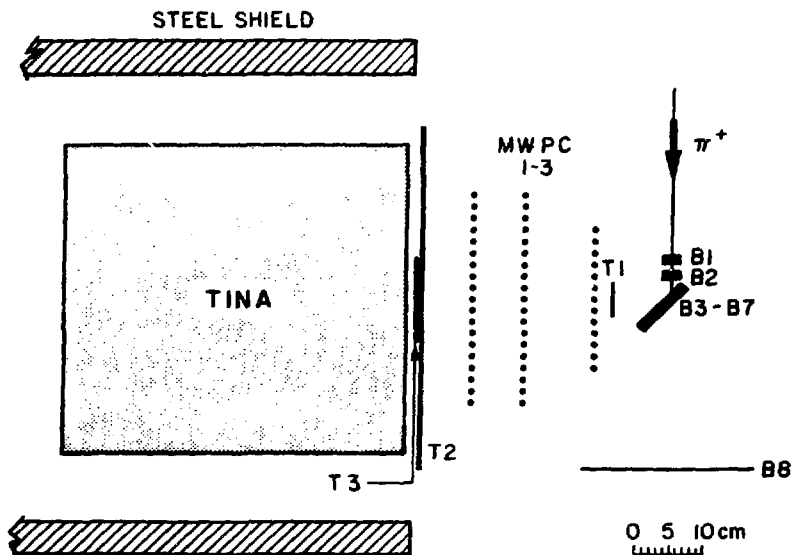


Fig. 1

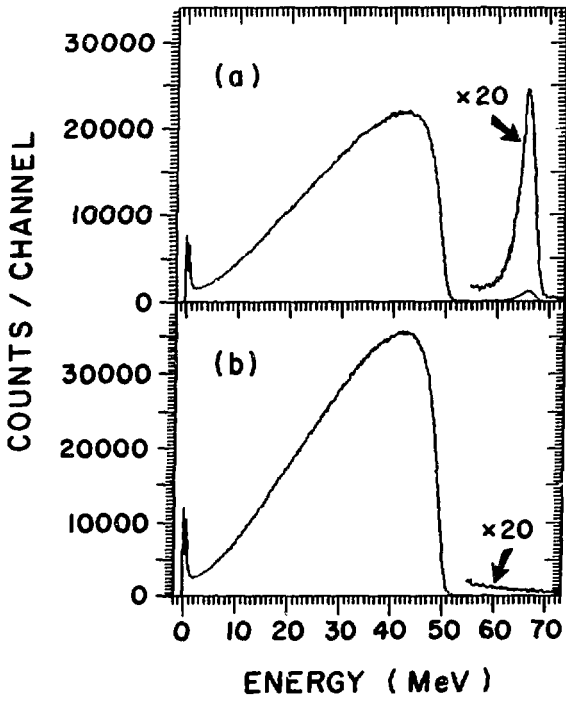


Fig. 2

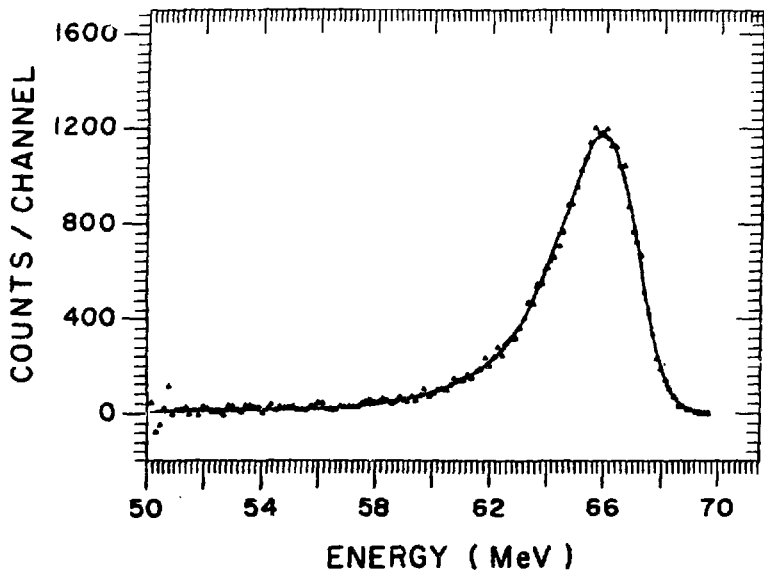


Fig. 3

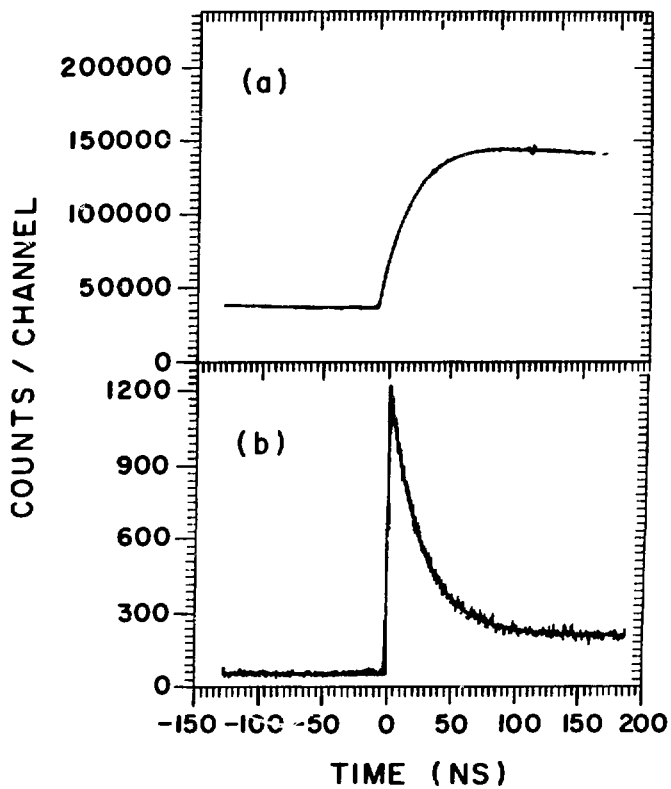


Fig. 4